(Received 18 May 2025, Accepted 18 July 2025, Scheduled 30 July 2025)

Highly Isolated Compact Dual-Band MIMO Antenna Using Stubs, Slots and Neutralization Line for 5G Wi-MAX and WLAN Applications

Amit A. Deshmukh[1], Shankar D. Nawale[2], Vijay R. Kapure[3, 4], Shubhangi A. Deshmukh[4], Mahadu A. Trimukhe[5], and Rajiv K. Gupta[6, *]

[1] *S. K. N. Sinhgad College of Engineering, Pandharpur, Solapur, India*
[2] *N. B. Navale Sinhgad College of Engineering, Solapur, India*
[3] *Xavier Institute of Engineering, Mahim, India*
[4] *Mumbai University, India*
[5] *Bharati Vidyapeeth (Deemed to be University), DET (Off Campus), Navi Mumbai, India*
[6] *Department of ECE, Ramrao Adik Institute of Technology, D. Y. Patil Deemed to be University, Navi-Mumbai, India*

ABSTRACT: A highly isolated MIMO antenna is designed using a neutralization line (NL), stubs, and slots for 5G, Wi-MAX, and WLAN operations. A quarter circular ring monopole is modified to have a circular outer shape and a polygon inner shape. Thickness of the monopole is reduced to decrease the electromagnetic (EM) coupling between the higher order modes and to obtain dual band characteristics. A two-element MIMO antenna is designed. High isolation is achieved by combining isolation techniques of neutralization line with stubs and slots. Isolation > 20 dB is achieved with stubs and slots in ground plane. Without altering the overall dimensions, isolation is improved from 20 dB to 30 dB by using an NL in the MIMO structure that uses slots and stubs in the ground plane as isolation techniques. $S_{11} < -10$ dB over 2.9–3.9 GHz and 5.6–6.2 GHz and $S_{12} < -30$ dB over 3.3–3.9 GHz, and $S_{12} < -40$ dB over 5.6–6.2 GHz covering 5G, Wi-MAX, V2X, and WLAN bands are obtained. The antenna has stable radiation patterns. ECC (Envelope Correlation Coefficient) < 0.002, DG (Diversity Gain) close to 10 dB, and MEG (Mean Effective Gain) about 0 dB satisfy MIMO specifications. The compact, low-cost antenna on a 30×50 mm FR4 substrate is simple to design and fabricate. These features make it a suitable candidate for 5G, Wi-MAX, and WLAN applications.

1. INTRODUCTION

High data rate, large channel capacity, and low latency are the driving force behind the rapid growth of wireless communication technologies. MIMO antenna offers a solution to these requirements as it operates over parallel communication channels [1]. However, due to size constraints, the performance of MIMO system is adversely affected by the mutual coupling between antenna elements. Researchers have employed different techniques and analyzed diverse solutions to mitigate mutual coupling issues in MIMO antennas [2, 3]. Electromagnetic bandgap (EBG) structures, metamaterial-based elements, and meandering line resonators effectively isolate multiple antenna elements [4–7]. Compact dual-band and tri-band MIMO antennas for LTE, WLAN, Wi-MAX, and 5G standards [8–13] have been reported. Neutralization lines are incorporated to reduce mutual coupling in ultra-wideband (UWB) and multi-band MIMO antennas [14–17]. A neutralization line reduces mutual coupling because out-of-phase currents over the path connecting the elements cancel the near fields. A 2-element microstrip antenna with slots and neutralization lines is designed in [18].

Pattern diversity and ground plane modification techniques have improved isolation in compact antennas [19–21]. Slots and stubs are employed in pie-shaped, G-shaped, hook-shaped, crescent shaped, and swastika-shaped multiband antennas to reduce mutual coupling in [22–26]. Coplanar waveguide feed is modified in a simple asymmetrical coplanar strip (ACS), and orthogonal polarization diversity is employed to design a compact MIMO antenna in [25, 26]. A tri-band MIMO antenna consisting of a thin L strip and a quarter circular monopole is designed with a parasitic element. Slots and stubs are incorporated in the ground plane to improve isolation [27]. A MIMO antenna on a flexible thin substrate is designed for wearable and portable communication systems for 5G networks applications [28]. The substrate flexibility with orthogonal polarization diversity offers improved isolation performance. A T-shaped stub acts as a decoupling structure between two circular shaped monopole antenna elements in [29]. A two-element MIMO planar inverted F-shape antenna (PIFA) is designed with an L-shaped slot in the ground plane to achieve isolation > 21 dB [30].

A compact UWB MIMO antenna is designed with extended F-shaped stubs in ground plane to achieve isolation > 25 dB [31]. A defective ground structure (DGS) is designed to improve isolation > 15 dB in [32]. Various isolation techniques used in MIMO antennas have been investigated in [33, 34]. DGS and complementary split ring resonators

* Corresponding author: Rajiv Kumar Gupta (rajivmind@gmail.com).

TABLE 1. Optimized parameters' dimension of the antenna.

Parameters	L	W	D	GSL	GSW	S1	S2	S3	SL1
dimensions (mm)	30	50	19.5	16	5	3	1	2	13
Parameters	SW1	SL2	SW2	Lg	Wf	PS	RW	NL	NW
dimensions (mm)	1.5	22	1	11.1	3	3.3	9.6	31.9	0.5

(C-SRRs) are designed to reduce mutual coupling in [35]. Isolation $>$ 22 dB is achieved for a dual-band antenna using metasurface in [36].

Wide-band antennas are useful and sometime unavoidable, as single antenna is used to cover multiple bands. However, the radiation patterns vary over large bandwidth and result in poor signal/noise ratio (SNR). The wideband antenna may cause interference with other devices operating over narrow bands in the vicinity. To mitigate these drawbacks, we have designed a compact dual-band MIMO antenna with isolation $>$ 30 dB over two bands by combining isolation techniques of slots, stubs, and NL.

In this paper, a dual-band MIMO antenna covering 3.3–3.9 GHz and 5.6–6.2 GHz frequency bands for 5G (3.3–3.8 GHz), Wi-MAX (3.4–3.6 GHz), V2X (5.75–5.925 GHz), and WLAN (5.725–5.875 GHz) applications is presented. Its two elements are placed side by side and are mirror image monopoles. The high isolation is realized by incorporating slots and stubs in the ground plane and an NL connecting the two radiating elements. The radiation patterns of antenna in two bands are stable. $S_{12} < -30$ dB and ECC < 0.002 with DG close to 10 dB are obtained which qualify the structure for MIMO applications. The dimensions of the antenna having $>$ 30 dB isolation are smaller than that of the reported antennas.

2. ANTENNA GEOMETRY, EVOLUTION AND DESIGN THEORY

Electromagnetic (EM) coupling between higher-order modes, which get excited in a monopole radiator, results in ultra-wide bandwidth. The wideband higher-order modes of a monopole resonate at different but nearby frequencies. The resonant frequencies of higher order modes and their impedance bandwidth (IBW) depend on the shape and dimensions of monopole radiator and ground plane as well as dielectric constant and thickness of substrate. These attributes of monopole antenna have led to innumerable monopole structures. However, UWB and wideband radiators interfere with narrowband devices. To overcome this problem, band-notch UWB antennas or multi-band antennas are designed. Branches of different lengths, widths, and shapes are traditionally designed, each having its own resonant frequency and BW.

A UWB or wideband monopole can operate as dual or multi-band antenna if the coupling between higher order modes is reduced by (a) decreasing the thickness, (b) removing the symmetrical portion of radiating element, (c) increasing the gap between radiating monopole and ground-plane, and (d) decreasing the dimensions of ground plane. Thereafter, the structure can be modified and optimized to operate over the desired bands.

These monopoles may constitute MIMO structures. The isolation can be improved by placing the elements, so that they are mirror images of each other, to neutralize/cancel the near field responsible for the mutual coupling. Slots are incorporated in the ground plane so that surface waves traverse long path, and thus mutual coupling due to surface waves decreases. The stubs act as decoupling structures and reflect the near fields responsible for mutual coupling. Besides slots and stubs, a neutralization line connecting the two radiators is also incorporated. The out-of-phase currents over the neutralization line connecting the elements cancel the fields that cause the mutual coupling between the elements. Without altering the overall dimensions, isolation is improved significantly from 20 dB to 30 dB by using an NL in the MIMO structure that uses slots and stubs in the ground plane as isolation techniques.

Figures 1 and 2 show the geometry and fabricated antenna, respectively. An antenna of dimension 30 mm $\times$ 50 mm is designed on an FR4 substrate (1.6 mm thickness, $\varepsilon r = 4.4$, and $\tan\delta = 0.02$) using (a) slots and stubs and (b) slots, stubs, and NL. The MIMO structure consists of two monopoles separated by 19.5 mm. The parameters' dimensions are listed in Table 1.

Antenna's different evolution stages are depicted in Fig. 3. In antenna 'A-1', a quarter circular ring monopole is modified to have a circular outer shape and an 11-side polygon inner shape. The thickness of monopole is reduced to decrease EM coupling between the higher order modes and to obtain dual-band characteristics. In uniform thick annular ring monopole, the surface current density decreases from feed line to the top edge. Therefore, the surface area is increased from feed line to the top edge in 'A-1' to enhance the surface current density and effective current path length. It decreases resonating frequency resulting in miniaturization/compact size. 'A-1' on a 30 mm $\times$ 28 mm substrate offers $S_{11} < -10$ dB over 2.8–3.9 GHz and 6.7–13.2 GHz. The ground plane is extended to accommodate the second element in 'A-2'. The ground plane dimensions affect the impedance matching, resonant frequency, and BW of different modes. A mirror image of the first element is placed at 19.5 mm in 'A-3'. $S_{11} < -10$ dB is obtained over 3.1 GHz–4.0 GHz and 6.5 GHz–9 GHz, while $S_{12} < -20$ dB and < -8 dB are obtained over two bands, respectively. The impedance matching as well as isolation is not satisfactory.

A wide slot is etched between the two elements to increase the surface wave path length in 'A-4'. The surface current magnitude is maximum at the edge near the radiating monopole. By etching a slot, the path length increases, and amplitude of surface waves decreases, resulting in improvement in isolation. $S_{11} < -10$ dB and $S_{12} < -25$ dB are obtained over 3.1–

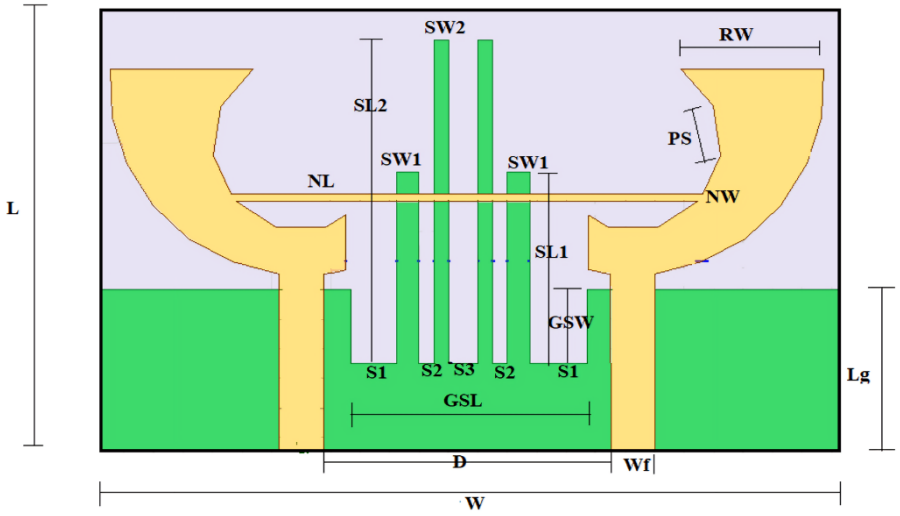

FIGURE 1. MIMO antenna geometry using isolation techniques of slots, stubs and NL.

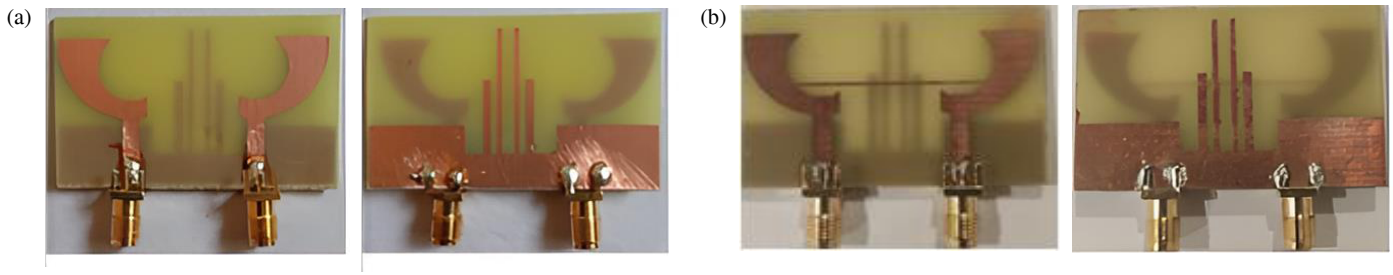

FIGURE 2. Fabricated MIMO antennas using (a) slots and stubs (b) slots, stubs and NL.

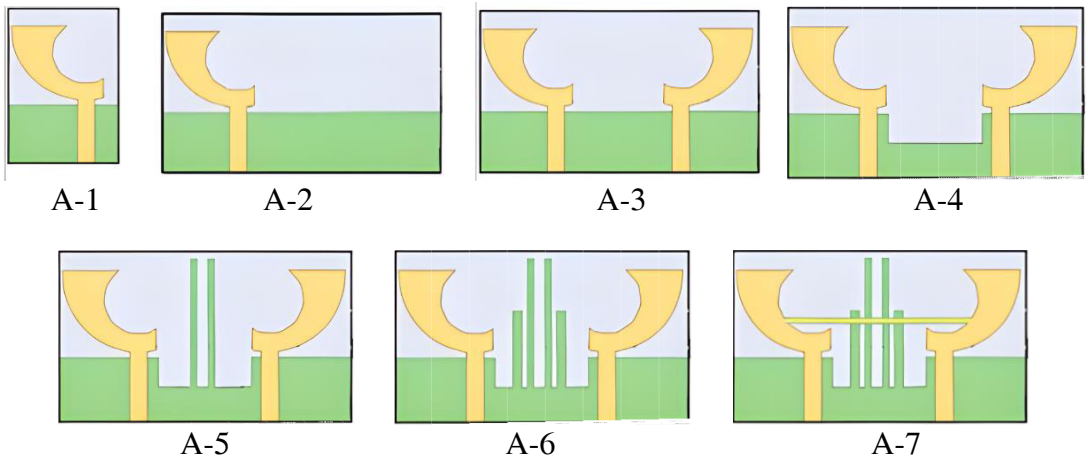

FIGURE 3. Evolution stages of MIMO antenna.

3.9 GHz. However, impedance matching and isolation degrade significantly in the upper band.

In 'A-5', two stubs with length more than that of radiating monopoles are added protruding from the wide slot in the ground plane. These stubs provide decoupling path to the surface waves and also reflect the near fields. The resonant frequencies decrease, and isolation improves due to stubs. $S_{11} < -10$ dB and $S_{12} < -25$ dB are obtained over 3.0–4.0 GHz while $S_{11} < -10$ dB and $S_{12} < -36$ dB are obtained over 5.9–6.2 GHz. Two shorter stubs are added in 'Ant 6'. $S_{12} < -20$ dB and $S_{12} < -30$ dB are obtained over 3.4–3.9 GHz and 5.9–6.2 GHz. In 'A-7', an NL connecting the two radiators is incorporated. The out-of-phase currents over the neutralization line connecting the elements cancel the fields causing mutual coupling between the elements. The resonant frequencies of two bands decrease, and isolation improves due to NL. $S_{11} <$

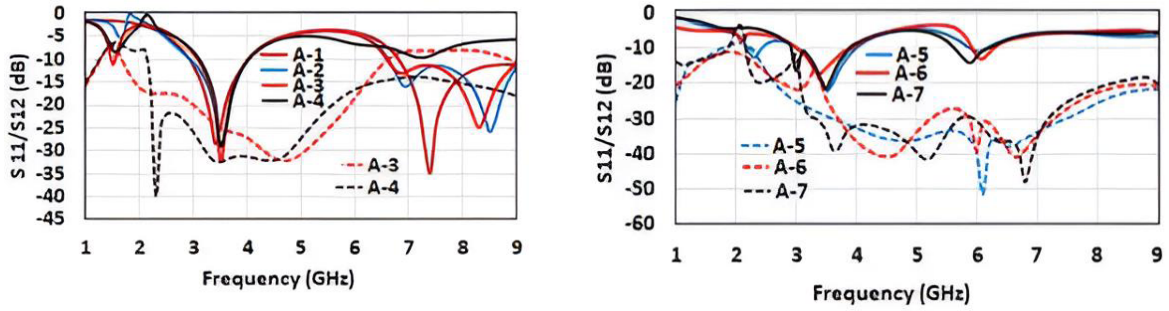

FIGURE 4. S parameters of evolution stages of MIMO antenna.

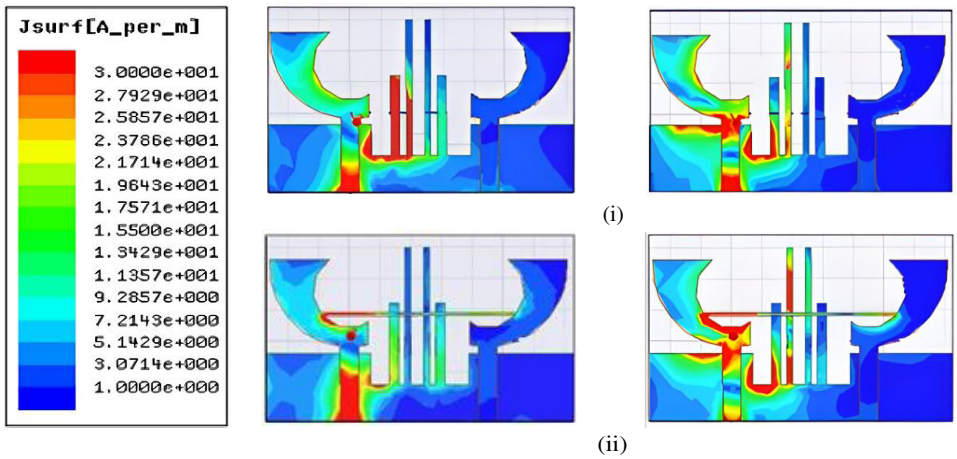

FIGURE 5. Scalar surface current density MIMO antennas using (i) slots and stubs and (ii) slots, stubs and NL in two operating bands. (a) 3.6 GHz, (b) 5.9 GHz.

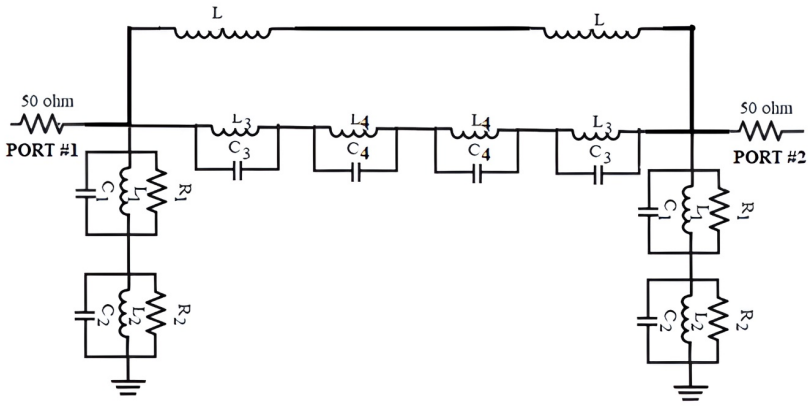

FIGURE 6. Equivalent circuit of proposed MIMO antenna using isolation techniques of slots, stubs and NL.

-10 dB and $S_{12} < -30$ dB are obtained over 3.3–3.9 GHz and 5.6–6.2 GHz for 5G (3.3–3.8 GHz), Wi-MAX (3.4–3.6 GHz) V2X (5.75–5.925 GHz) and WLAN (5.725–5.875 GHz) applications. The structures are optimized at each stage. Fig. 4 shows S parameters of different stages of antenna.

The scalar surface current densities of 'A-6' and 'A-7'are depicted in Fig. 5. In 'A-6', there is significant current in the shorter stub and longer stub in lower band as compared to 'A-7', and therefore, NL significantly improves isolation in 'A-7'. The NL provides an additional path, and surface current is concentrated towards the left element which results in decrease in resonant frequency in lower band and improvement in isolation. The effective surface current density on NL is more in upper band which results in considerable decrease in resonant frequency in upper band as compared to lower band. The radiation patterns become more directive in upper band as antenna operates in higher mode as compared to lower band where it operates in fundamental mode.

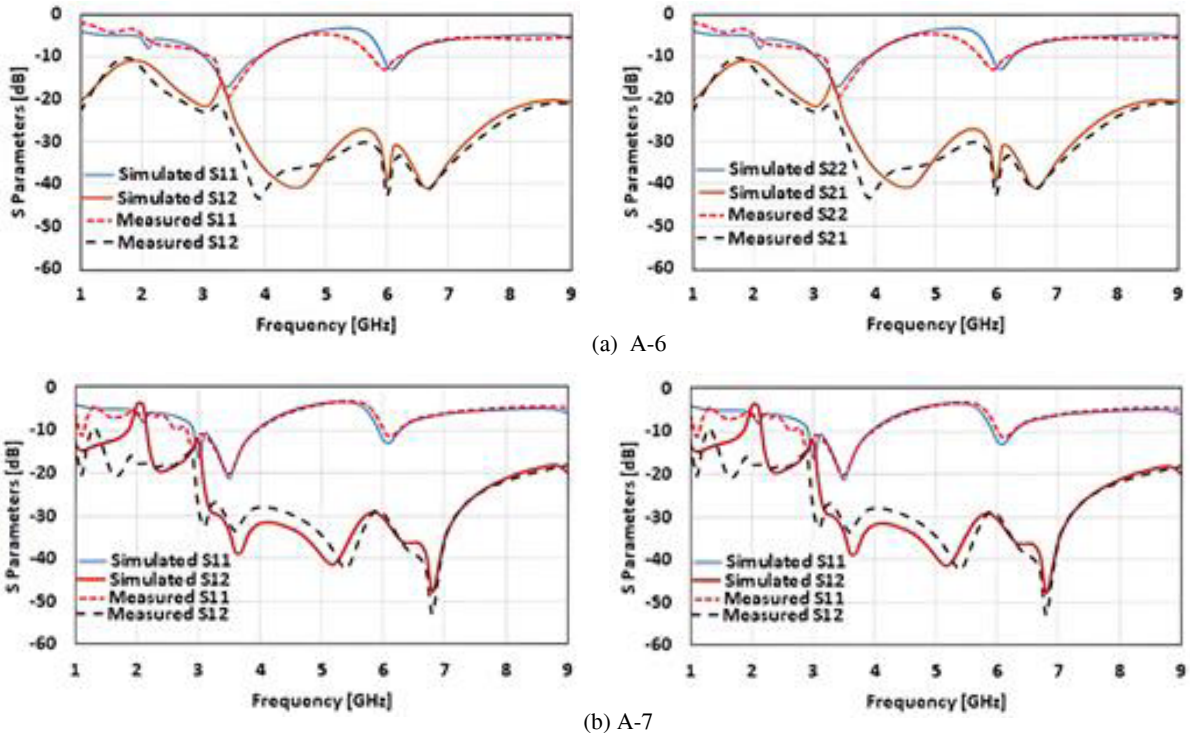

(a) A-6

(b) A-7

FIGURE 7. S-parameters of antennas using (a) slots and stubs (b) slots, stubs and NL. (i) Port 1 excited, (ii) Port 2 excited.

The working of dual bands and isolation between two elements of MIMO antenna can be analyzed with the help of the equivalent circuit shown in Fig. 6. The dual-band operation of monopole antenna is equivalent to two parallel circuits of R_1-L_1-C_1 and R_2-L_2-C_2 connected in series. The two monopole elements are fed through 50 Ω microstrip transmission line at port 1 and port 2 [37]. Stubs and slots in ground plane form band-stop filters. They are represented by the parallel combination of L_3-C_3 and L_4-C_4. These band-stop filters do not allow the surface current or near fields to couple with the second element and thus provide isolation > 20 dB over two bands. The metallic NL connecting the two monopole radiators is equivalent to inductor L. The current in NL flows from element 1 to 2, but it is neutralized by an opposite current flowing from element 2 to 1. Thus, NL cancels the near fields responsible for mutual coupling and enhances the isolation significantly by 10 dB. As a result, NL in combination with stubs and slots offers > 30 dB isolation over the desired bands. Since the two monopoles are identical and symmetrical, the equivalent circuit is also symmetrical at port 1 and port 2.

3. MEASURED RESULTS AND ANALYSIS

3.1. S-Parameters

The antenna is fabricated using advanced photolithography techniques. An Agilent 9916A network analyzer is used to measure the S parameters and to compare it with simulated S parameters (Fig. 7) of prototype antennas (Fig. 2). One port is excited, and the other port is terminated. In the desired bands, S_{11} and $S_{22} < -10$ dB and S_{12} and $S_{21} < -30$ dB are obtained. The measured results closely agree with the simulated ones. The discrepancy in measured and simulated results may be attributed to connector loading and substrate parameters.

3.2. Radiation Patterns and Diversity Performance

The radiation patterns of the MIMO antenna are shown in Fig. 8, in which one port is excited and other terminated using a matched impedance. The radiation patterns are mirror images of each other when port 1/port 2 is excited while the other port is terminated. The co-polar and cross-polar components of radiation patterns in E and H planes at 3.2, 3.4, 3.6, and 3.8 GHz covering lower band and 5.6, 5.8, 6.0, and 6.2 GHz covering upper band are shown in Fig. 8. There is little variation in radiation pattern over two bands. Thus, the antenna radiates stable omnidirectional fields. The antenna diversity is confirmed through identical mirror images of the radiation patterns when 'port 1' or 'port 2' is excited. The simulated and measured gains and antenna efficiencies are shown in Fig. 9. The maximum gain of 1.4 dBi with 73% efficiency and 4.1 dBi with 84% efficiency are obtained in two bands. Higher gains in upper frequency band can be attributed to increase in effective aperture area with frequency.

Diversity performance evaluation of the MIMO antenna is achieved by analyzing ECC, DG, and MEG values. The communication channel between two points follows the isolation defined by ECC. The mechanism analyzes mutual field interference that occurs from one antenna to another when both function together. ECC is determined under uniform multipath indoor environment. The simulated and measured ECC < 0.002 in desirable bands, illustrated in Fig. 10, depict diversity performance of MIMO antenna.

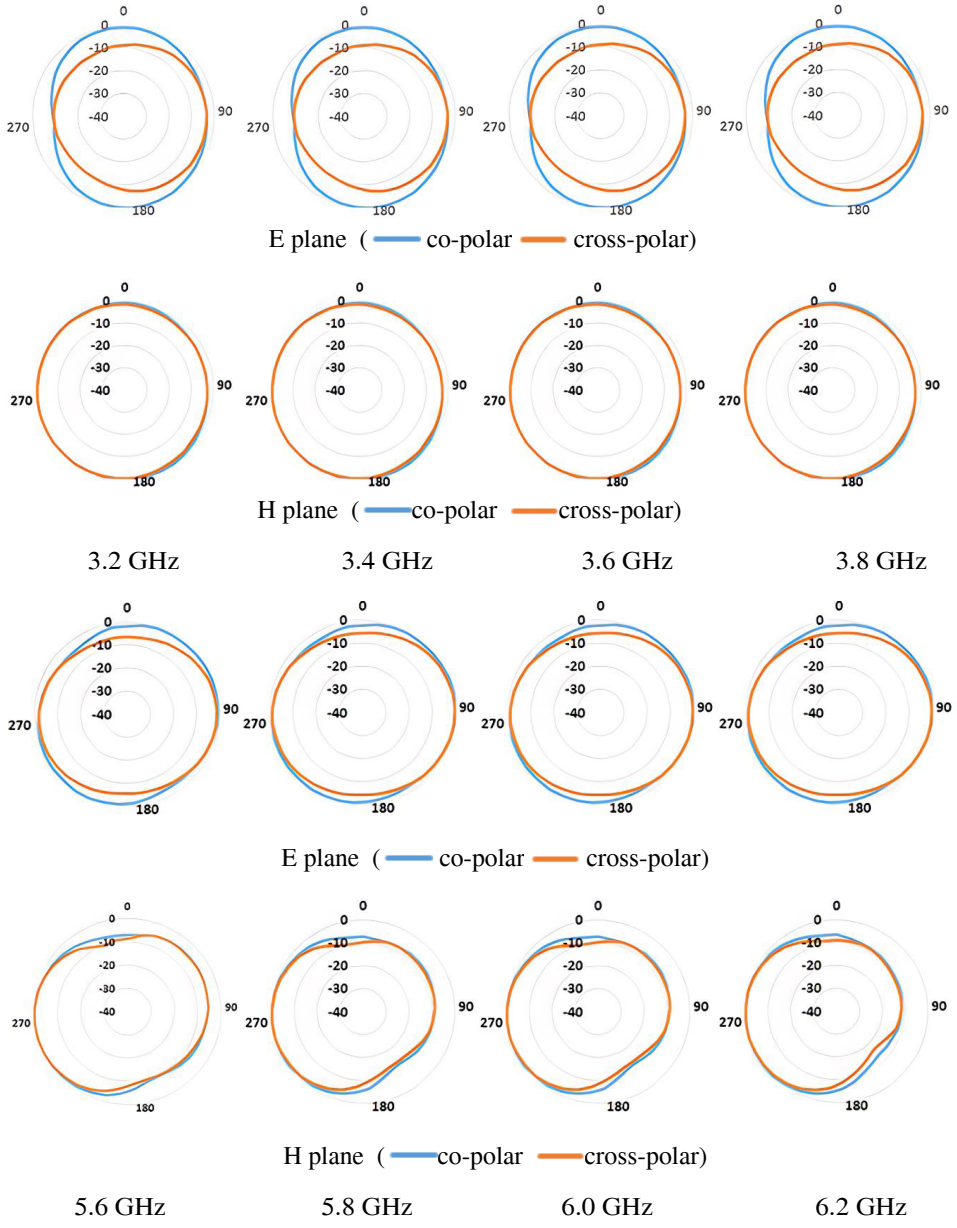

FIGURE 8. Radiation patterns of proposed MIMO antenna using slots, stubs, and NL.

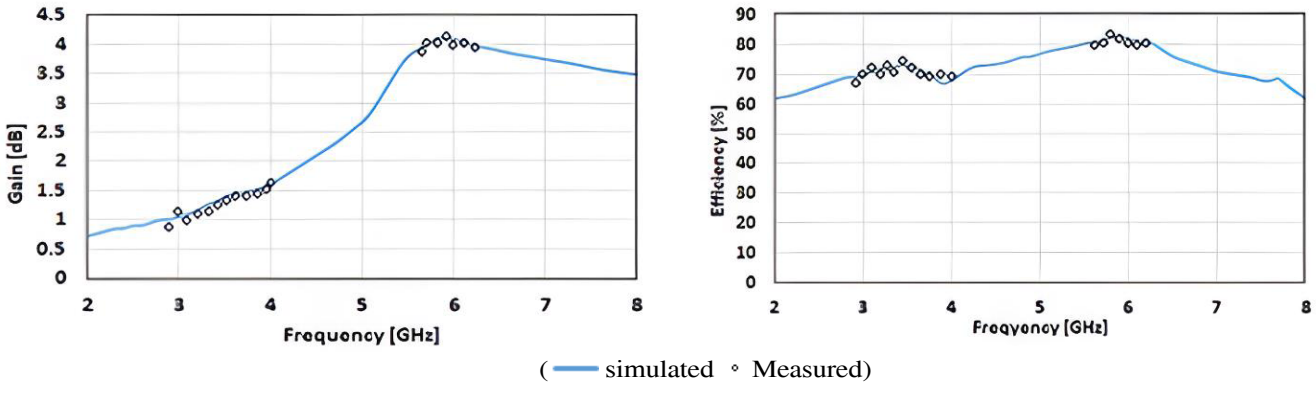

FIGURE 9. Antenna peak gain and efficiency of proposed antenna using Slots, stubs and NL.

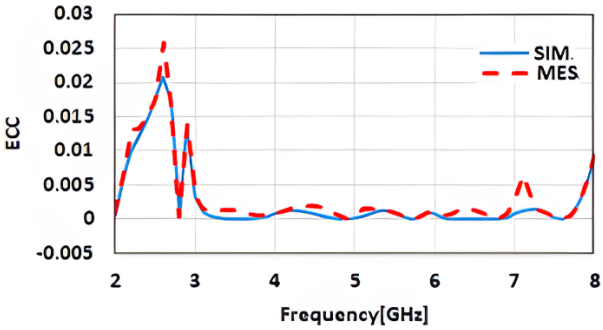

FIGURE 10. Envelope correlation coefficient.

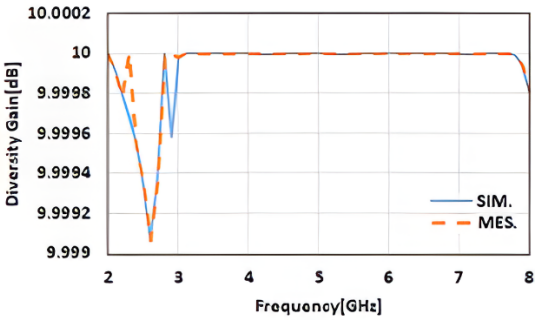

FIGURE 11. Diversity gain.

TABLE 2. Comparison with reported MIMO structures.

Ref.	Isolation-Techniques	Bands (GHz)	Isolation (dB)	Antenna size $(\lambda_0 \times \lambda_0)\lambda_0^2$	ECC	DG
[6]	C-SRRs microstrip antennas	2.34–2.47 3.35–3.64	31 20	$0.34 \times 0.203 = 0.069$	0.05	9.4
[7]	meander-line decouple-structure	2.4–2.48 5.15–5.83	9 25	$0.48 \times 0.48 = 0.2304$	0.08	9.8
[9]	Elliptical slot and parasitic strip	3.2–3.8 5.7–6.2	20 20	$0.32 \times 0.28 = 0.089$	0.03	9.5
[10]	Slots, stub and parasitic element	3.41–3.60 4.76–5.04	29 41.4	$0.44 \times 0.64 = 0.282$	0.005	9.7
[11]	Elliptical decouple-structure	3.2–6	15	$0.64 \times 0.43 = 0.275$	0.003	9.5
[14]	Slots, Stubs, NL	3.7–39 5.6–5.9	15 15	$0.37 \times 0.37 = 0.137$	0.001	10
[16]	NL between Microstrip Antenna elements	2.2–3.1 5.7–6.5	29 48	$0.44 \times 0.29 = 0.1276$	0.001	9.9
[17]	NL	3.1–11.7	16.5	$0.475 \times 0.475 = 0.226$	0.01	9.6
[19]	Spatial Orientation	2.4–2.52, 3.66–4, 4.62–5.52	30.5 18.5	$0.212 \times 0.664 = 0.1407$	0.001	9.9
[22]	Spatial orientation, Stubs and slots	2.82–8.21 9.8–12.42	18 16	$0.244 \times 0.376 = 0.0917$	0.002	9.99
[24]	Decoupling T-structure	1.85–3.63 1.73–2.28	17.2 22.4	$0.284 \times 0.185 = 0.053$	0.003	9.9
[25]	hook shaped decoupling, ACS fed	2.25–2.4 4.7–6.3	15 15	$0.375 \times 0.375 = 0.1406$	0.0025	9.9
This Work	Stubs, slots and Neutralization line	2.9–3.9 5.56–6.25	31 41	$0.29 \times 0.48 = 0.139$	0.001	9.9

Equation (1) is used to calculate DG from correlation coefficient values. DG of approximately 10 dB (Fig. 11) in bands of interest demonstrates good diversity performance.

$$\mathrm{DG} = 10\sqrt{1 - |\,\mathrm{ECC}|^2} \tag{1}$$

The antenna needs to fulfill MEG requirement in addition to ECC defined in Equation (2).

$$\mathrm{MEG}_i/\mathrm{MEG}_j = 1 \tag{2}$$

$$\mathrm{MEG}_i = \frac{1}{4\pi}\int_0^{4\pi} |\mathbf{F}_i(\theta,\phi)|^2 P(\theta,\phi)\, d\Omega \tag{3}$$

where $P(\theta, \varphi)$ is uniform, assuming ideal propagation. MEG can also be calculated using S-parameters.

Figure 12 depicts the simulated (S) and measured (M) MEG1, MEG2, as well as MEG1/MEG2 plots. MEG1 shares virtually the same characteristics as MEG2 while their ratio MEG1/MEG2 remains about 0 decibel throughout the desired bands. The simulated and measured total active reflection coefficients (TARCs) are plotted in Fig. 13 using Equation (4).

$$\mathrm{TARC} = \sqrt{\frac{|\mathbf{S}_{11}+\mathbf{S}_{12}|^2 + |\mathbf{S}_{21}+\mathbf{S}_{22}|^2}{2}} \tag{4}$$

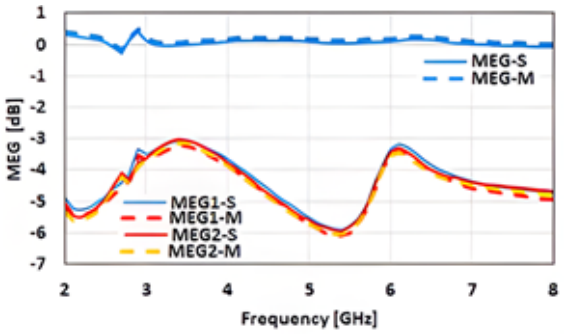

FIGURE 12. MEG of proposed antenna.

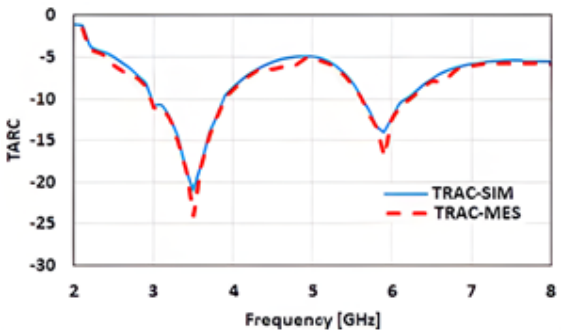

FIGURE 13. TARC of proposed antenna.

4. COMPARISON WITH REPORTED ANTENNAS

Table 2 lists the comparison of our antenna with reported antennas in terms of technique, electrical size, bandwidth, isolation, and ECC. Different techniques and their combinations and effect on isolation, ECC, and DG are listed in Table 2. Structures in [6] and [16] are microstrip antenna (MSA) MIMO structures while the rest are monopole MIMO antennas. Refs. [7, 11, 17, 19, 25] have larger dimensions and low isolation than the proposed structure. The antenna in [10] has comparable isolation but occupies double area than our antenna. Structures in [6, 9, 14, 22, 24] have smaller dimensions but offer significantly low isolation. The antenna in [16] has comparable dimensions and isolation, but it is an MSA MIMO antenna while the proposed structure is a monopole MIMO antenna. Both the structures use NL to achieve high isolation. The proposed antenna is simple to design and fabricate, low in cost, offers stable radiation patterns, and satisfies all MIMO diversity parameters and standards.

5. CONCLUSION

A low cost and simple-to-design, MIMO structure consisting of two monopole antenna elements is designed. The monopole is designed from a circular monopole. A quarter circular monopole is designed, and an 11-sided regular polygon slot is etched from it. The design decreases the thickness of monopole radiator which decreases the mutual coupling between higher-order modes. It results in a dual-band antenna. The surface area of the radiating element is gradually increased from near the feed to the top which increases effective surface current and decreases resonant frequency. Simple techniques of stubs and slots in ground plane are employed to achieve 20 dB isolation. Isolation is improved to 30 dB by incorporating a neutralization line connecting the two monopole radiators. Thus, a highly isolated MIMO antenna is proposed using a neutralization line, stubs, and slots for 5G, Wi-MAX, V2X, and WLAN operations. Isolation $>$ 30 dB in lower 5G and Wi-MAX band and $>$ 40 dB in WLAN and V2X band is obtained. The proposed antenna offers stable radiation patterns and adheres to all diversity parameters and MIMO standards.

REFERENCES

[1] Jensen, M. A. and J. W. Wallace, "A review of antennas and propagation for MIMO wireless communications," *IEEE Transactions on Antennas and Propagation*, Vol. 52, No. 11, 2810–2824, 2004.

[2] Nadeem, I. and D.-Y. Choi, "Study on mutual coupling reduction technique for MIMO antennas," *IEEE Access*, Vol. 7, 563–586, 2019.

[3] Chouhan, S., D. K. Panda, M. Gupta, and S. Singhal, "Multi-port MIMO antennas with mutual coupling reduction techniques for modern wireless transreceive operations: A review," *International Journal of RF and Microwave Computer-Aided Engineering*, Vol. 28, No. 2, e21189, 2017.

[4] Naser-Moghadasi, M., R. Ahmadian, Z. Mansouri, F. B. Zarrabi, and M. Rahimi, "Compact EBG structures for reduction of mutual coupling in patch antenna MIMO arrays," *Progress In Electromagnetics Research C*, Vol. 53, 145–154, 2014.

[5] Veeramani, A., A. S. Arezomand, J. Vijayakrishnan, and F. B. Zarrabi, "Compact S-shaped EBG structures for reduction of mutual coupling," in *2015 Fifth International Conference on Advanced Computing & Communication Technologies*, 21–25, Haryana, India, 2015.

[6] Panda, A. K., S. Sahu, and R. K. Mishra, "A compact dual-band 2 × 1 metamaterial inspired MIMO antenna system with high port isolation for LTE and WiMax applications," *International Journal of RF and Microwave Computer-Aided Engineering*, Vol. 27, No. 8, e21122, 2017.

[7] Deng, J. Y., Z. J. Wang, J. Y. Li, and L. X. Guo, "A dual-band MIMO antenna decoupled by a meandering line resonator for WLAN applications," *Microwave and Optical Technology Letters*, Vol. 60, No. 3, 759–765, 2018.

[8] Hussain, R., M. U. Khan, and M. S. Sharawi, "An integrated dual MIMO antenna system with dual-function GND-plane frequency-agile antenna," *IEEE Antennas and Wireless Propagation Letters*, Vol. 17, No. 1, 142–145, 2018.

[9] Nirmal, P. C., A. Nandgaonkar, S. L. Nalbalwar, and R. K. Gupta, "A compact dual band MIMO antenna with improved isolation for Wi-Max and WLAN applications," *Progress In Electromagnetics Research M*, Vol. 68, 69–77, 2018.

[10] Wang, W., Y. Wu, W. Wang, and Y. Yang, "Isolation enhancement in dual-band monopole antenna for 5G applications," *IEEE Transactions on Circuits and Systems II: Express Briefs*, Vol. 68, No. 6, 1867–1871, 2021.

[11] Bait-Suwailam, M. M., T. Almoneef, and S. M. Saeed, "Wideband MIMO antenna with compact decoupling structure for 5G wireless communication applications," *Progress In Electromagnetics Research Letters*, Vol. 100, 117–125, 2021.

[12] Pradeep, P., J. S. Kottareddygari, and C. S. Paidimarry, "A compact 4 x 4 peace-shaped wideband MIMO antenna for sub-6 GHz 5G wireless applications," *International Journal of Microwave & Optical Technology*, Vol. 17, No. 5, 508, 2022.

[13] Kadu, M., R. Pawase, P. Chitte, and V. S. Ubale, "Compact dual-band antenna design for sub-6 GHz 5G application," *Bulletin of Electrical Engineering and Informatics*, Vol. 13, No. 3, 1656–1666, 2024.

[14] Jha, P., A. Kumar, D. Sahu, and N. Sharma, "Isolation enhancement of two element MIMO antenna based on neutralization technique," in *2023 3rd International Conference on Advancement in Electronics & Communication Engineering (AECE)*, 355–359, GHAZIABAD, India, 2023.

[15] Yu, Y., X. Liu, Z. Gu, and L. Yi, "A compact printed monopole array with neutralization line for UWB applications," in *2016 IEEE International Symposium on Antennas and Propagation (APSURSI)*, 1779–1780, Fajardo, PR, USA, 2016.

[16] Babu, K. V. and B. Anuradha, "Design of Wang shape neutralization line antenna to reduce the mutual coupling in MIMO antennas," *Analog Integrated Circuits and Signal Processing*, Vol. 101, No. 1, 67–76, 2019.

[17] Dkiouak, A., M. E. Ouahabi, S. Chakkor, M. Baghouri, A. Zakriti, and Y. Lagmich, "High performance UWB MIMO antenna by using neutralization line technique," *Progress In Electromagnetics Research C*, Vol. 131, 185–195, 2023.

[18] Yu, Y., L. Yi, X. Liu, and Z. Gu, "Compact dual-frequency microstrip antenna array with increased isolation using neutralization lines," *Progress In Electromagnetics Research Letters*, Vol. 56, 95–100, 2015.

[19] Dileepan, D., S. Natarajan, and R. Rajkumar, "A high isolation multiband MIMO antenna without decoupling structure for WLAN/WiMAX/5G applications," *Progress In Electromagnetics Research C*, Vol. 112, 207–219, 2021.

[20] Yang, M. and J. Zhou, "A compact pattern diversity MIMO antenna with enhanced bandwidth and high-isolation characteristics for WLAN/5G/WiFi applications," *Microwave and Optical Technology Letters*, Vol. 62, No. 6, 2353–2364, 2020.

[21] Khade, A., M. A. Trimukhe, S. M. Verulkar, and R. K. Gupta, "Dual band MIMO antenna with high isolation for GSM and WLAN applications," *Progress In Electromagnetics Research C*, Vol. 136, 189–198, 2023.

[22] Kakkar, A., M. R. Tripathy, A. K. Singh, *et al.*, "A novel compact two element MIMO antenna with pie shaped slot structure for dual band applications," in *2017 Progress in Electromagnetics Research Symposium — Fall (PIERS — FALL)*, 336–341, Singapore, Nov. 2017.

[23] Yahya, L. S., L. S. Yahya, and K. H. Sayidmarie, "A crescent-shaped monopole MIMO antennas with improved isolation for dual-band WLAN applications," *Progress In Electromagnetics Research C*, Vol. 117, 115–127, 2021.

[24] Tiwari, R. N., P. Singh, S. Pandey, R. Anand, D. K. Singh, and B. K. Kanaujia, "Swastika shaped slot embedded two port dual frequency band MIMO antenna for wireless applications," *Analog Integrated Circuits and Signal Processing*, Vol. 109, No. 1, 103–113, 2021.

[25] Naidu, P. V., D. Maheshbabu, A. Saiharanadh, A. Kumar, N. Dudi, L. Sumanji, and K. A. Meerja, "A compact four-port high isolation hook shaped ACS fed MIMO antenna for dual frequency band applications," *Progress In Electromagnetics Research C*, Vol. 113, 69–82, 2021.

[26] Naidu, P. V., A. Saiharanadh, D. Maheshbabu, A. Kumar, and N. Vummadisetty, "Design and performance analysis of g-shaped compact ACS fed 4-port MIMO antenna for triple frequency band applications," *Progress In Electromagnetics Research C*, Vol. 112, 55–68, 2021.

[27] Khade, A., M. Trimukhe, S. Jagtap, and R. K. Gupta, "A circular sector with an inverted L shaped monopole antenna for triband applications," *Progress In Electromagnetics Research C*, Vol. 118, 177–186, 2022.

[28] Achariparambil, A., K. K. Indhu, R. A. Kumar, K. Neema, and C. K. Aanandan, "Ultra-wideband quad element MIMO antenna on a flexible substrate for 5G and wearable applications," *Progress In Electromagnetics Research C*, Vol. 126, 143–155, 2022.

[29] Khan, M. K., Q. Feng, and Z. Zheng, "Experimental investigation and design of UWB MIMO antenna with enhanced isolation," *Progress In Electromagnetics Research C*, Vol. 107, 287–297, 2021.

[30] Biswal, S. P. and S. Das, "Two-element printed PIFA-MIMO antenna system for WiMAX and WLAN applications," *IET Microwaves, Antennas & Propagation*, Vol. 12, No. 14, 2262–2270, 2018.

[31] Konade, S. and M. Dongre, "Compact two-port MIMO antenna with high isolation for UWB applications," *Iranian Journal of Electrical & Electronic Engineering*, Vol. 20, No. 2, 1–9, 2024.

[32] Pradeep, P., K. J. Sankar, and C. S. Paidimarry, "Design of a compact wideband two-port MIMO antenna for NR 5G sub-6 GHz band wireless applications," *Wireless Personal Communications*, Vol. 138, No. 2, 1193–1210, 2024.

[33] Prakash, P., G. Manoj, and J. S. Immanuel, "A comprehensive review: Advances in MIMO antenna for IOT application," *Wireless Personal Communications*, Vol. 136, No. 2, 793–826, 2024.

[34] Jagadeesan, K. and P. Manickavelu, "Isolation enhancement techniques in MIMO antenna systems: A survey," *Telecommunications and Radio Engineering*, Vol. 83, No. 11, 1–12, 2024.

[35] Manage, P. S., U. Naik, and V. Rayar, "Compact design of MIMO antenna with split ring resonators for UWB applications," *Nano Communication Networks*, Vol. 41, 100512, 2024.

[36] Feng, H., Z. Wang, W. Nie, and M. Yang, "High-gain dual-band metasurface MIMO antenna for enhanced 5G and satellite applications," *Progress In Electromagnetics Research C*, Vol. 156, 13–22, 2025.

[37] Khade, A., M. Trimukhe, S. Verblkar, and R. K. Gupta, "Miniaturization of printed rectangular monopole antenna by using slots for triple band applications," *Progress In Electromagnetics Research C*, Vol. 130, 155–167, 2023.